Macromolecules 1991, *24*, 1041–1049

Oriented Films from Polymeric Amphiphiles with Mesogenic Groups: Langmuir–Blodgett Liquid Crystals?

Thomas L. Penner* and Jay S. Schildkraut

Corporate Research Laboratories, Eastman Kodak Company, Rochester, New York 14650

Helmut Ringsdorf and Andreas Schuster

Institute of Organic Chemistry, University of Mainz, D-6500 Mainz,
Federal Republic of Germany

Received May 11, 1990

ABSTRACT: Langmuir–Blodgett films prepared from preformed amphiphilic polymers containing mesogenic chromophores ("amphotropic" polymers) exhibit a phase change to a less ordered state on heating. This reversible transition occurs at the same temperature as the onset of liquid-crystal formation in the bulk material. Spectroscopic and ellipsometric characterization provides quantitative information on the chromophore orientation in the films as a function of temperature. These results show a highly ordered aggregated structure at room temperature with a sharp transition to a more mobile state at about 60 °C. The chromophores are then no longer aggregated and exhibit a broader distribution of orientations, although on the average they are still quite highly aligned. This behavior is similar to liquid-crystal formation in bulk materials and opens the possibility of inducing monodomain formation in Langmuir–Blodgett films. For the polymer studied in most detail, the liquid-crystal-like condition persists in the films up to the highest temperature studied, ca. 150 °C in contrast to the bulk material that becomes isotropic by 84 °C. The ordered aggregated structure is recovered reversibly on cooling even from the highest temperature without loss of film integrity, demonstrating an enhanced stabilization in the Langmuir–Blodgett film environment.

1. Introduction

The use of preformed polymers in the preparation of monolayer films at the air–water interface and their subsequent deposition as Langmuir–Blodgett (LB) films has been recognized for some time as having the potential for improving the properties of such films relative to conventional monomeric amphiphiles.[1-3] In recent years the synthesis of specially designed amphiphilic polymers has allowed the fabrication of such films with retention of side-group orientation and relatively facile deposition properties.[4-6] In particular, the use of flexible spacer groups to decouple side-chain ordering from backbone structure has resulted in close-packed ordered polymeric monolayer films.[4,7,8] Although initially the polymer side groups were hydrocarbon and fluorocarbon chains, the most recent examples contain bulkier chromophoric groups.[9-11] It is of special interest that in some cases such chromophores act as mesogenic units, imparting liquid-crystalline properties to bulk samples of the amphiphilic polymers.[11,12] This leads to the possibility of introducing liquid-crystal-like behavior in polymeric Langmuir–Blodgett films. The advantages of using materials that increase thermal stability in Langmuir–Blodgett films are well recognized.[1,13] The benefits to be gained from the incorporation of liquid-crystal-like behavior are potentially as important but perhaps not as obvious. Within the field of Langmuir–Blodgett research, it is generally recognized that domains or two-dimensional microcrystals form in most films that are deposited from solid monolayer phases.[14,15] Thus, although they can show a high degree of molecular orientation perpendicular to the film plane, the in-plane structure is rather local.[16] This is undesirable for a number of properties such as optics or in-plane conductivity. Deposition of monolayer films from more fluid phases is usually very difficult, requiring special techniques, and the resulting structures are generally not highly ordered.[17,18] It would be desirable to be able to reorient films after they have been deposited as solid phases. This requires the introduction of molecular mobility into the transferred films by a process such as heating, without permanently destroying the order and structure. Conventional amphiphiles fail to provide sufficient mobility along with the necessary stability. By a combination of amphiphilic and mesogenic elements to create bifunctional "amphotropic" molecules,[12] it may be possible to induce mobility in the Langmuir–Blodgett films.[19,20] By further incorporation of such amphotropic units in a polymeric structure in which the functional units are attached to but decoupled from the backbone,[11] it may be possible to provide thermal stability.[12] Such a concept is shown schematically in Figure 1.

We report here on the characterization of monolayers at the air–water interface and of Langmuir–Blodgett films prepared from such amphotropic polymers. Since relatively little has been reported on the packing and order of polymeric LB films with covalently attached chromophores, we have used polarization spectroscopy at ultraviolet–visible and infrared wavelengths to obtain such information. We have also investigated the temperature-dependent properties of the films, using ellipsometry as well as polarization spectroscopy as tools to monitor thermally induced changes. These experiments address both a search for phase changes in the films and their stability at high temperature.

2. Experimental Section

2.1. Materials. 2.1.1. Monomer Synthesis. All compounds were synthesized at the University of Mainz. The chiral azobenzene monomer was prepared according to Scheme I. The exact procedures will be reported in more detail in a later communication.[21]

2.1.2. Polymerization. The homo- and copolymerization with 2-hydroxyethyl acrylate (HEA) was performed according to published procedures.[7] The polymers were characterized by TLC and ^{1}H NMR and FTIR spectroscopy. The compositions of the random copolymers given in structure I are the ratios of the comonomer feeds and do not reflect the exact values in the polymers. Judging from the results of the ^{1}H NMR analysis, the actual HEA comonomer content is somewhat higher for copolymers $x = 5$, 10 but could not be determined accurately.

2.2. Characterization. 2.2.1. Bulk Properties. Phase transitions were observed by differential scanning calorimetry (DSC) with a Perkin-Elmer DSC 2C instrument. Visual characterization of the liquid-crystalline properties of the bulk

0024-9297/91/2224-1041$02.50/0

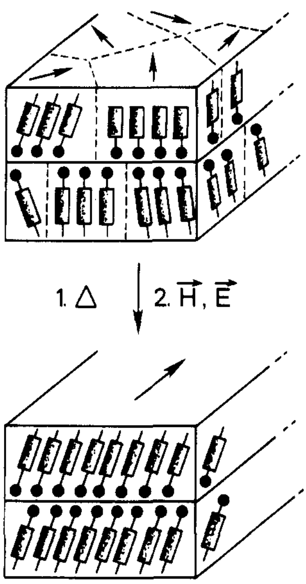

Figure 1. Conceptual picture of the conversion of a multidomain structure into a monodomain through the field-induced alignment of a LB film of an amphotropic polymer.

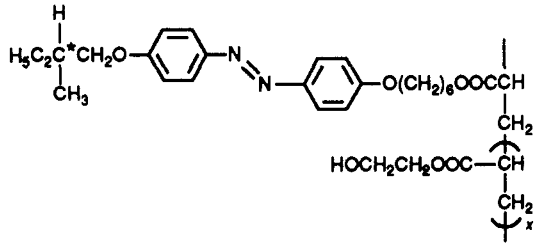

I, x = 0, 1, 5, 10

material was done with an Olympus Vanox transmission polarizing microscope equipped with a DPLAN 10P0 objective or a Leitz Ortholux IIPOL-BK polarizing microscope, both equipped with a Mettler FP52/FP5 hot stage and controller. Langmuir-Blodgett multilayer films deposited on aluminum or quartz substrates were examined with an Olympus BH2 microscope under dark-field conditions, using various NEOSPLAN objectives (5-100×).

2.2.2. Monolayers. Monolayers were characterized by using a computer-controlled KSV Series 2200 film balance containing a Wilhelmy plate pressure sensor system. The polymeric amphiphiles were spread as chloroform solutions in concentrations of about 0.5-1 mg/mL (approximately (3-10) × 10^{-4} mol/L). Surface pressure was recorded versus area per repeat unit for each polymeric amphiphile at room temperature without additional temperature control. Compression rates varied from 5 to 12 Å^2/(repeat unit min). Throughout all experiments a plain water subphase was used. The water was purified by passing a reverse osmosis treated feed through a Milli-Q water purification system (Millipore Corp.).

2.2.3. Langmuir-Blodgett Multilayers. Langmuir-Blodgett multilayers were also deposited from a pure Milli-Q water subphase at room temperature. Deposition pressure, compression, and deposition speeds were varied to optimize film transfer to substrates. After compression to the deposition pressure, the monolayers were given 30-45 min to equilibrate prior to transfer.

2.2.4. Substrates. Depending on the particular experiment, a variety of substrates have been used. These include glass and fused silica slides, silicon wafers, and aluminum evaporated as a 2000-Å film on cleaned silicon wafer substrates by electron beam heating. All substrates used in this investigation were hydrophilic.

Substrate preparation and cleaning procedures depended on the particular substrate. Glass and quartz slides were soaked in chloroform for 1 day and in cold chromic acid solution for at least another day before they were rinsed with distilled water. They were treated with a mixture of nitric acid, sulfuric acid, and water (1:3:6) for another day, rinsed with distilled and Milli-Q water, and dried with nitrogen gas. Glass substrates were plain 1 in. × 3 in. Fisher precleaned microscope slides, and quartz slides were Suprasil-fused silica optical windows from Helma (1/2 in. × 7/4 in.). Silicon substrates were cut from standard-damage (100) silicon wafers purchased from Wacker-CHemitronic GmbH. They were soaked in a mildly alkaline detergent solution (Deconex 12 PA, Balzers Optical Group) for five minutes and rinsed with Milli-Q water at room temperature (15 min) and for an additional 10 min with water vapor. They were then dipped in isopropyl alcohol and degreased with toluene vapor (15 min). An alternate procedure involved intensive scrubbing of the silicon surface with a soft brush soaked in Deconex 12 PA and subsequent rinsing with large amounts of distilled and Milli-Q water. These substrates were also dried in a stream of nitrogen gas. Similar results were obtained with both cleaning procedures. Neither removes the ca. 20-Å of native silicon oxide that exists on the surface. No additional mechanical or chemical cleaning was used on the evaporated aluminum surfaces. For all materials each substrate was exposed to an argon plasma (Harrick PDC-3XG Plasma Cleaner) for 5-10 min immediately before Langmuir-Blodgett film deposition.

Scheme I

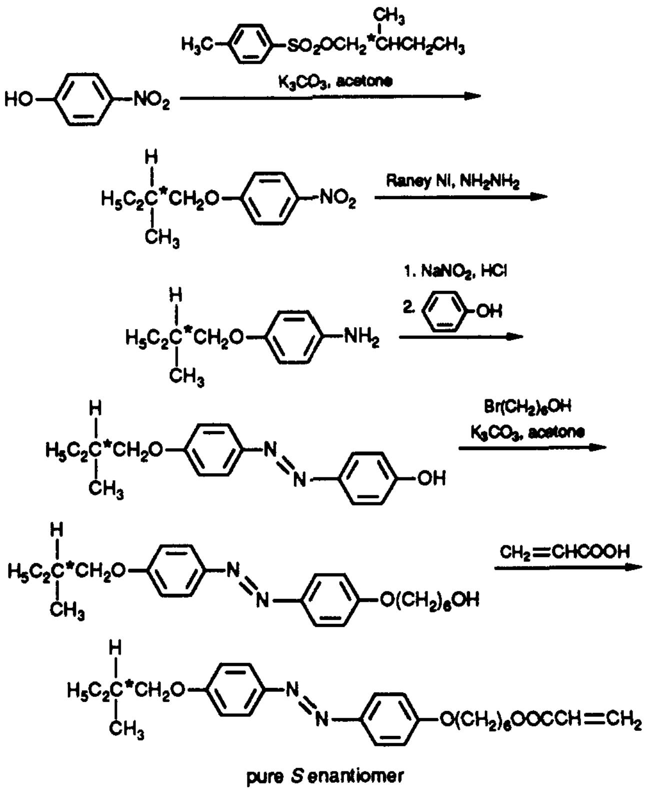

2.2.5. Spectroscopy. Ultraviolet absorption spectra were recorded with a double-beam Varian Cary 2290 spectrophotometer equipped with a depolarizer, a Glan-Taylor polarizer (Harrick Scientific Corp.), and a sample stage that could be rotated for variations of the incident beam angle. An IBM-PC was used for storage and manipulation of spectra. Heating experiments were carried out in an insulated box constructed of polycarbonate polymer with quartz transmission windows placed in the spectrometer's sample compartment, a platinum resistance thermal detector (RTD) probe thermometer, and two gas connections. The chamber was heated with hot nitrogen gas, produced in electrically heated copper tubing. The temperature of the sample could be controlled fairly accurately (±1 °C) by adjusting the gas flow rate through the chamber. Temperatures up to 100 °C could be obtained.

Fourier transform infrared (FTIR) experiments were performed with a Nicolet IR/44 FTIR instrument attached to an IBM-PC work station for data processing. A deuterated triglycine sulfate (DTGS) detector was operated at room temperature. To obtain a good signal-to-noise ratio at the chosen resolution of 4 cm^{-1}, 2000 scans were collected over about 20 min

Table I
Bulk Liquid-Crystalline Phase Transitions

compd	composition	phase-transition temperature,[a] °C
x = 0, homopolymer	1:0	g 68 c 76 s_1 95 s_2 106 i
x = 1, copolymer	1:1	c 59 s_1 76 s_2 89 i
x = 5, copolymer	1:5	g 13 c 57 s 84 i[b]
x = 10, copolymer	1:10	g 6 c 56 lc 75 i[b]

[a] g = glass transition, c = crystalline, s = smectic, lc = unspecified liquid crystalline phase, i = isotropic. [b] These clearing temperatures (i.e., transition to isotropic liquid) were based on visual observation.

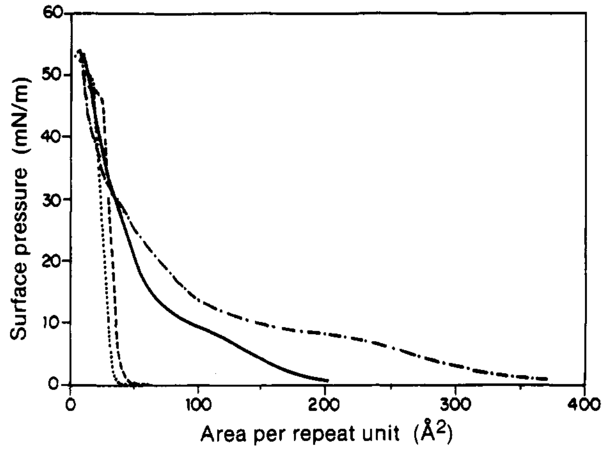

Figure 2. Pressure–area isotherms of copolymer series I on pure water subphase: x = 0 (· · ·), x = 1 (- - -), x = 5 (—), x = 10 (- · -).

and averaged. A single diamond-germanium polarizer (Harrick Scientific Corp.) provided polarized light.

A Harrick variable-angle reflection accessory, modified to allow sample heating, was used for grazing angle reflection[22] (GIR) measurements. The heating unit was similar to that reported by Schlotter and Rabolt.[23] A thermocouple connected to an Omega HH52 digital thermometer monitored the temperature on the aluminum substrate surface. Incident light was p polarized.

Transmission FTIR spectra were obtained at room temperature at normal incidence on silicon wafers polished on both sides.

2.2.6. Ellipsometry. Most ellipsometric measurements were made with a computer-controlled Gaertner L116B-Auto Gain ellipsometer equipped with a He–Ne laser (wavelength = 632.8 nm, 3 mW/cm^2) and a rotating analyzer. The angle of incidence was set to 70° for all experiments. An aluminum block heater could be mounted on the ellipsometer stage.

Refractive index determinations within the chromophore absorption band were carried out on a Rudolph manual ellipsometer equipped with a quartz–halogen tungsten lamp and a wavelength-isolating interference filter from Ditric Optics Inc. (wavelength = 350 nm, fwhm bandwidth = 10 nm).

3. Results

3.1. Bulk Properties. Bulk properties of the polymers were investigated by polarizing microscopy and DSC analysis. Table I lists the bulk phase-transition temperatures measured by DSC and their assignments based on visual observation. All polymers, even copolymers with high amounts of nonmesogenic hydrophilic HEA comonomer, show liquid-crystalline phases. Note that the transition from the crystalline to liquid crystalline phase is at about 60 °C and that clearing to an isotropic liquid phase occurs below 100 °C for all but the homopolymer. Additional characterization of bulk liquid-crystalline properties of these and related polymers is underway.[24]

3.2. Monolayers. Figure 2 shows surface pressure versus area isotherms measured for the series of copolymers, x = 0, 1, 5, 10. The areas were calculated on the basis of the monomeric repeat unit for each polymer, assuming that the final comonomer ratio in each case is the same as in the synthetic feedstock. A progression of film properties with the ratio of hydrophilic comonomer is seen. For the homopolymer and 1:1 copolymer only a single condensed phase is evident. For the two polymers with greater hydrophilic comonomer content, a more compressible, liquidlike region is observed that is longer for the polymer with greater hydrophilic monomer content, although at higher pressures these two materials also exhibit low compressibility, i.e., solid analogue phases. The collapse pressure for all these compounds is very similar with the possible exception of the 1:1 copolymer that appears to collapse at slightly lower pressure. Within the uncertainty of the actual composition of the various polymers the "molecular" areas at collapse do not differ significantly.

3.3. Multilayers. 3.3.1. Film Deposition. As indicated in the Experimental Section, Langmuir–Blodgett multilayers were deposited on a variety of hydrophilic substrates depending on the particular experiment. Although all four compounds formed stable monolayers at the air–water interface, the polymers x = 0, 1 did not deposit quantitatively as multilayers. Optical microscopy of glass slides onto which these compounds had been deposited showed incomplete coverage in the form of a striped pattern. On the other hand, copolymers x = 5, 10 deposited readily on both up and down strokes (Y deposition) on all hydrophilic substrates examined. A pressure of 30 mN m^{-1} was chosen for film deposition. The optimum deposition rate on the upstroke was 4–5 mm/min and on the downstroke was 1–3 mm/min for x = 5 and 2–5 mm/min for x = 10. For both materials the upstroke transfer ratio was 1.0 ± 0.1 and for the downstroke it was 0.7 ± 0.1. These values were reproducible on different kinds of substrates. Ellipsometric measurements showed variations of less than 1–2% in film thickness over several square centimeters of substrate area. Films deposited on aluminum-coated silicon and measured by GIR FTIR showed a linear increase in absorbance (defined as $-\log R/R_0$, where R and R_0 are the reflectivities of the aluminized substrate measured with and without the LB film, respectively) with the number of bilayers deposited for a variety of bands.[11] The high compressibility of polymer x = 10 made it difficult to introduce enough material onto the water surface to allow the deposition of more than a few layers from a single spreading. Thus most of the spectroscopic and thermal experiments were done with the polymer x = 5. More limited experiments with the polymer x = 10 indicated spectroscopic and thermal behavior similar to that reported in more detail for x = 5. It was critical to good deposition of these two polymers that a sufficient equilibration time was allowed after compression to the desired surface pressure before deposition was begun. In addition, at least 15 min of drying time in air was allowed between successive immersion and withdrawal cycles to prevent delamination of the previous monolayer from the substrate.

3.3.2. Ultraviolet Spectroscopy. Figure 3 shows orthogonally polarized transmission spectra of the polymer x = 5 deposited on fused silica substrates. For the polarization labeled $\parallel$ the substrate was oriented in the spectrometer so that the light impinged on it normal to the film plane and with the dipping direction parallel to the electric field of the polarized light. The polarization labeled $\perp$ is rotated by 90° from this direction. Figure 3a gives the spectra of the LB film as deposited. In Figure 3b the sample has been heated to 90 °C and then returned to room temperature prior to measurement. The former shows a substantial dichroism with the $\parallel$ absorbance, indicated by $A_{\parallel}$, greater than $A_{\perp}$. The spectra after heat treatment show essentially no dichroism. By monitoring the polarization ratio as a function of temperature, we

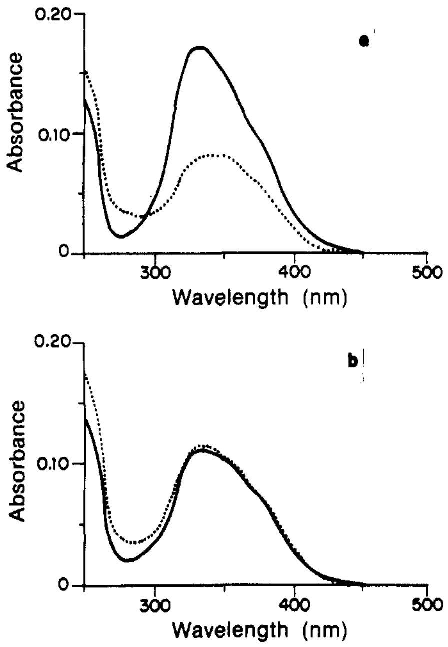

Figure 3. Polarized ultraviolet absorption spectra of a nine-layer Langmuir–Blodgett film of copolymer $x = 5$ at normal incidence: (a) unheated sample; (b) room-temperature spectrum after heating to 90 °C; $A_{\parallel}$ (—), $A_{\perp}$ (· · ·).

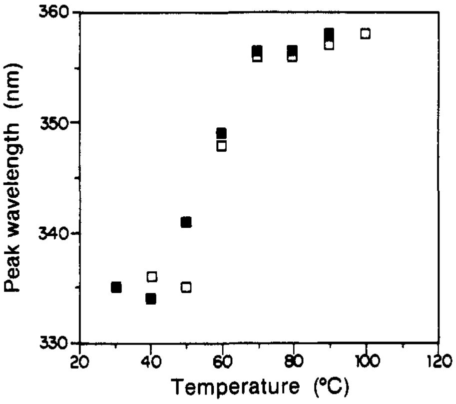

Figure 4. Temperature dependence of absorption peak wavelength for copolymer $x = 5$: first heat cycle (□); second heat cycle (■).

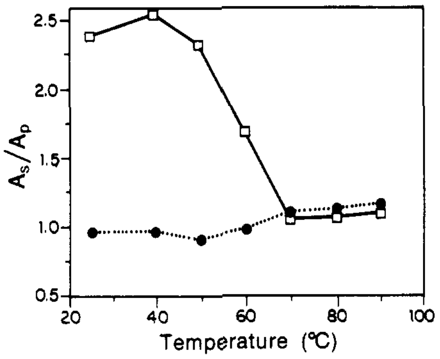

Figure 5. Temperature dependence of ultraviolet absorption peak dichroism for copolymer $x = 5$ at an angle of incidence of 45° and with electric field of s-polarized light parallel to dipping direction: first heat cycle (□); second heat cycle (●).

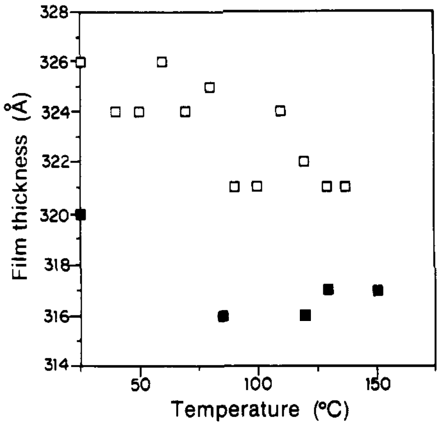

Figure 6. Temperature dependence of thickness of a nine-layer Langmuir–Blodgett film of copolymer $x = 5$ on aluminized silicon substrate, monitored ellipsometrically: first heat cycle (□), second heat cycle (■).

observed that a change in dichroic ratio $A_{\parallel}/A_{\perp}$ from 2.5 to 1.0 occurred between 50 and 70 °C.

Figure 4 plots the absorption peak position as a function of the temperature at which the spectrum was measured. The peak position remains essentially constant at 335 nm up to 50 °C, whereupon a sudden shift to 355 nm occurs. At higher temperatures the band again remains essentially unchanged at least up to 100 °C, the highest temperature used. After cooling to room temperature, the band returned to the original peak position. Subsequent heating cycles followed essentially the same dependence of peak position on temperature.

In addition to these absorption experiments measured at normal incidence, a series of spectra were measured as a function of temperature with the light incident on the sample at 45°. In this case, the light polarized with the electric field perpendicular to the plane defined by the incident and reflected light beams is designated as s polarized and with the electric field parallel to this plane is designated as p polarized. The substrate was oriented so that the electric field of s-polarized light was parallel to the sample dipping direction. The change in dichroic ratio with temperature is plotted in Figure 5 for two successive heating cycles of the same sample. The spectra for the unheated film show a large dichroic ratio that falls rapidly with a midpoint at about 60 °C, as is the case for normal incidence. After cooling, a second heat cycle shows a small reversible change in dichroism, also at about 60 °C.

3.3.3. Ellipsometry. Ellipsometry was also measured as a function of temperature on a nine-layer sample of copolymer $x = 5$ deposited onto an aluminized silicon substrate. These measurements were performed at the 632.8-nm wavelength of a He–Ne laser using a fixed refractive index of 1.50. The results of two successive heating cycles are shown in Figure 6. The initial film thickness was 326 Å. A small gradual drift to lower apparent thickness with increasing temperature was observed, but no noticeable break occurs in the temperature range where the dichroic ratio and absorption peak position change rapidly. The overall thickness loss of 3–4% was largely irreversible on cooling of the sample. On a second heating to 150 °C the film thickness again decreased slightly, to 317–316 Å. To some extent the thickness measurements are dependent on the length of time the sample was maintained at high temperature. Thus holding the film at 155 °C for 2 h caused a further decrease in film thickness to 311 Å.

In addition to this conventional ellipsometry at a nonabsorbed wavelength we also performed ellipsometry at a wavelength where the azobenzene chromophore absorbs. As discussed below, to use linear dichroism measured by absorption spectroscopy quantitatively, it is necessary to know both the imaginary part of the complex refractive index (which could be calculated from absorption data) and also the real part at the resonance wavelength of absorption. With an ellipsometric wavelength of 350 nm,

Table II
Assignment of Infrared Bands of Copolymer $x = 5$

peak location, cm^{-1}	band assignment	peak location, cm^{-1}	band assignment
3700–3100	$\nu(OH)^a$	1254	$\nu(CO)^d$
3000–2800	ν_s, $\nu_a(CH_2, CH_3)^b$	1175	$\nu(COC)^a$
1740	$\nu(C{=}O)^a$	1082, 1036	$\nu(COH)^a$
1601, 1582	$\nu(C{=}C)^c$	843	$\delta(CH)^e$

[a] Band assignments follow those given in refs 6, 25, and 26. [b] ν_s and ν_a are symmetric and antisymmetric stretching modes, respectively. Specific assignments have not been made due to extensive overlap of CH_2 and CH_3 bands of similar intensity. [c] This is the $A_1\omega$ mode consisting of in-plane ring vibrations polarized along the long axis of the azobenzene chromophore.[27] [d] Aryl CO stretch.[27] [e] Aromatic CH out-of-plane bending.[27]

values of $n = 1.58 \pm 0.01$ and $k = 0.07 \pm 0.01$ were obtained for a 37-layer LB film (1347 Å thick). The value of n was found to be insensitive to orientation of the film relative to the light beam, but k varied with orientation as a result of in-plane chromophoric orientation. The quoted value of k was obtained after sample annealing above 60 °C, which removed this anisotropy.

3.3.4. Infrared Spectroscopy. Infrared spectra of Langmuir–Blodgett films were measured in two different configurations, transmission at normal incidence and grazing incidence reflection. Table II gives a partial assignment of selected vibrations.[25–27] Infrared transmission spectra at normal incidence were measured on a 35-layer film. During deposition two wafers were sandwiched together so the deposition occurred only on one side of each. Spectra with light polarized parallel and perpendicular to the dipping direction were determined as in the case of the ultraviolet spectra. The sample was then heated to 150 °C on a hot plate outside the spectrometer chamber and remeasured after cooling to room temperature. Prior to heating, most vibrational bands showed extensive in-plane dichroism, with the exception of carbonyl and saturated hydrocarbon stretching bands. For example, a band at 1601 cm^{-1} assigned to the azobenzene chromophore has an infrared dichroic ratio $A_{\parallel}/A_{\perp} = 2.1$. After heating, dichroism was absent in the normal-incidence transmission for all bands.

In the case of GIR spectra, nine-layer films were deposited onto aluminized silicon substrates. Grazing-angle reflection measurements were made as described in the literature[22,25] using an empirically optimized incidence angle, nominally 79°. The heater incorporated into the variable-angle reflection attachment allowed spectra to be recorded directly at different temperatures. Figure 7 compares spectra measured at 150 °C and room temperature, the latter obtained subsequent to cooling, i.e., after the first heating–cooling cycle. Variable differences in intensities are apparent in many bands.

Figure 8 shows a comparison of a GIR spectrum measured for a nine-layer sample and a transmission spectrum obtained for the 35-layer film on silicon. In both cases spectra shown were obtained after an initial heating–cooling cycle. The band intensities at approximately 3500 or 2900 cm^{-1} measured by the two techniques are fortuitously similar. It can be seen that bands such as those at 1582 and 1601 cm^{-1}, identified as aryl ring modes, lying along the long chromophoric axis (refer to Table II), or at 1254 cm^{-1}, due to aryl C–O stretch, are relatively more intense in the GIR spectrum than in transmission.

4. Discussion

4.1. Influence of Molecular Structure on Properties.

The progressive effect of hydrophilic comonomer content on the properties of these amphotropic polymers is evident in both bulk and monolayer form. As noted above, all polymers, even those with a high proportion of nonmesogenic hydrophilic HEA comonomer form bulk thermotropic liquid crystalline phases. Microscopy and preliminary X-ray results[24] show that polymers $x = 0$, 1, and 5 exhibit smectic phases, whereas for polymer $x = 10$ the nature of the liquid-crystalline phase is still unclear. With the exception of the homopolymer, the polymer composition has surprisingly little effect on the solid-to-liquid crystalline phase transition. On the other hand, the glass transition and the clearing transition to the isotropic phase occur at progressively lower temperature as the HEA comonomer content is increased. It should be emphasized that mesophase formation was unexpected in these vinyl copolymers. Generally, even small amounts of nonmesogenic groups within a liquid-crystalline polymer suppress formation of such phases.[28] In the present case the formation of smectic phases may be due to microphase separation, as reported for liquid-crystalline polysiloxanes.[28]

The occurrence of fluid-phase regions in the pressure–area isotherms at the air–water interface seen in Figure 2 for $x = 5$, 10 is indicative of less viscous as well as less-ordered films for these materials than for the $x = 0$, 1 polymers, at least at low pressure. This agrees with previous observations on polymers with hydrocarbon and fluorocarbon side chains.[7,8,29] On the other hand, the surface density or phase state of the polymers at higher surface pressure is not greatly influenced by the presence of the additional "spacer" comonomer,[7] indicating that the chromophore-containing side chain controls close-packing of the monolayer film in all cases. In fact, the polymers with greater hydrophilic comonomer content appear to have smaller surface areas per repeat unit at collapse. However, this is probably an artifact of the calculation of concentration, which was based on the assumption that the polymer compositions are the same as the synthetic feedstocks. Also the mechanical stability of the films as measured by collapse pressure is largely insensitive to comonomer content. The deposition behavior of the compounds is also consistent with the picture that the polymers with higher hydrophilic comonomer content are somewhat more fluid, although all four polymers were deposited at high pressures where the films exhibit low compressibility. Thus these materials have the very desirable characteristic of allowing certain film properties to be selectively engineered synthetically without altering others. This is achieved through decoupling of the molecular subunits that are responsible for the different properties.[7,30]

4.2. Spectroscopy and Molecular Orientation.

The properties of film structure, stability, and phase behavior of transferred LB films derived from this study all rely on the interpretation of spectroscopic data, including polarization effects. Therefore we will first discuss the interpretation of these results in terms of what they tell us about molecular order and orientation. This will focus largely on the azobenzene chromophore since this is a spectroscopically well-defined and identifiable structural unit whose behavior in the film is of particular interest.

A great deal has been published on the measurement and interpretation of experiments involving linear absorption of polarized light as a probe of molecular orientation.[31] In fact, some of the fundamental aspects of linear dichroism are still the subject of research.[32] Within the approximation of treating thin films of absorbing materials as continuous dielectric planar slabs, classical optics can be used to interpret the effects.[33,34] We recognize that a single technique such as polarized absorption cannot be used to describe the entire distribution of orientations

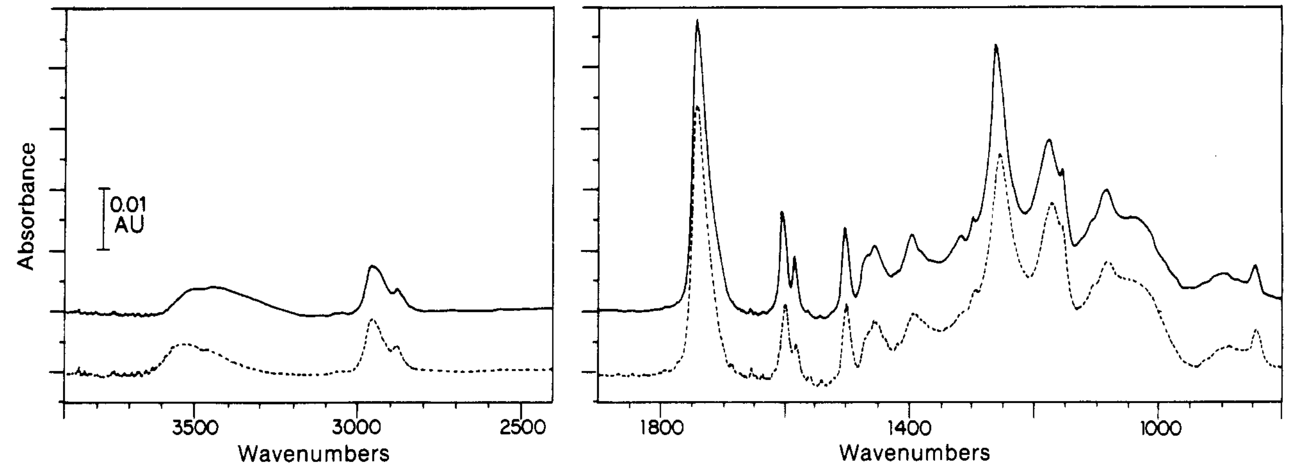

Figure 7. Grazing incidence reflection FTIR spectra of a nine-layer Langmuir–Blodgett film of copolymer $x = 5$ on aluminized silicon substrate measured at different sample temperatures: 25 °C (—), 150 °C (- - -). Curves are offset by 0.01 absorbance units (AU).

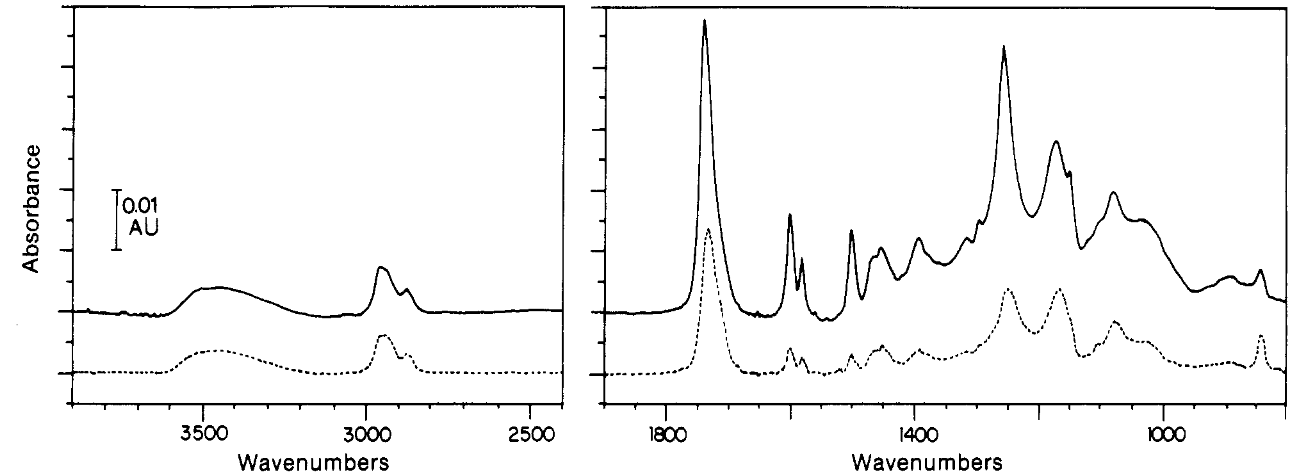

Figure 8. Comparison of FTIR spectra of Langmuir–Blodgett films of copolymer $x = 5$ measured in different modes: grazing incidence reflection of a nine-layer film on aluminized silicon (—), transmission spectrum of a 35-layer film on silicon (- - -). Curves are offset by 0.01 absorbance units (AU).

[$N(\theta)$] in a macroscopic ensemble of transition moments identified with that absorption, even under the assumption that such a distribution is uniaxial. In this case the dichroic absorption ratio A_s/A_p can be related to the average value of $\cos^2\theta$, symbolized by $\langle\cos^2\theta\rangle$, where θ is the polar angle between the transition moment and the uniaxial rotation axis.[35] Only under the additional assumption that θ has only one value [i.e., the distribution $N(\theta)$ is a δ function] is the value of θ directly obtainable from this average. Thus we will give our dichroism results in terms of $\langle P_2\rangle$, the second moment of the orientational-order parameter, where $\langle P_2\rangle = {}^1/_2(3\langle\cos^2\theta\rangle - 1)$. For illustrative purposes we will also quote an angle θ_{eff} defined as $\cos^{-1}(\langle\cos^2\theta\rangle^{1/2})$ derived from $\langle P_2\rangle$ on the (generally invalid) assumption that θ is single-valued. In the case of a technique such as GIR spectroscopy at a metallic surface one obtains data at only one polarization, in this case p.[36] Then to obtain an order parameter, it is generally necessary to have an external reference of the same material, such as an isotropic sample of known concentration or a film with the same molecular orientation but measured by transmission. Although such absolute experiments and the necessary optical calculations to relate the reflection and transmission techniques have been done,[37] results depend on assumptions such as invariance of extinction with the molecular environment. Such assumptions may be less valid for large chromophores such as azobenzene that are sensitive to environment and concentration effects than for weakly interacting groups such as hydrocarbons or carbonyls that have been analyzed previously. In addition, the calculations are also very sensitive to experimental conditions such as the precise grazing incidence angle. For these reasons we have chosen not to use our FTIR GIR and transmission experiments to extract absolute orientation parameters for the different bands. On the other hand, a qualitative comparison of GIR and transmission FTIR spectra as shown in Figure 8 gives an indication of the relative orientation of different molecular groups.[25] Thus the much diminished intensity of the bands at 1175, 1254, 1601, and 1740 cm^{-1} in the transmission spectrum compared to the GIR spectrum indicates that the transition moments of the corresponding groups (see Table II) are more oriented toward the film normal than are those of the OH and saturated hydrocarbon groups. More quantitative information can be obtained by monitoring changes in band intensities with conditions. For example, calculating ratios of order parameters from successive GIR spectra is relatively straightforward, allowing us to monitor how changing conditions such as temperature change orientation, as discussed below.

The substantial ultraviolet absorption dichroism observed for normally incident light shown in Figure 3a indicates that the azobenzene chromophore in the LB film of polymer $x = 5$ has a preferential orientation within the film plane. Such effects have been noted previously and are generally attributed to flow shear forces.[19,38,39] Indeed, since the transition moment for the π–π^* excitation of the para,para′-substituted azobenzene lies along the long molecular axis,[40] the dichroic ratio of 2.1 indicates that the chromophores are quite strongly aligned along the dipping direction. It is significant that this orientation within the film plane is irreversibly lost on mild heating of the film to above 60 °C. Subsequently the in-plane component of this transition moment is randomly distributed as evidenced by a dichroic ratio of 1.0, and further analysis of the polar orientation (i.e., normal to the film plane) can be done assuming uniaxial symmetry with respect to an axis normal to the film plane.

To do this one must solve the Fresnel equations for transmission through multilayer slabs of different refractive index. Since the calculation of linear dichroism of oriented thin films has been previously modeled by a number of authors,[32-34,41] we will outline our approach only qualitatively, indicating the general procedure, approximations, and significant departures from previous treatments. Our approach follows that detailed by Chollet[34] and generalized by Vandevyver et al.,[41] in which the imaginary part of the dielectric tensor is related to the polar angle, θ, so that under uniaxial symmetry the nonzero elements of the dielectric tensor ϵ_{zz} and $\epsilon_{xx} = \epsilon_{yy}$ can be expressed as functions of $\langle \cos^2 \theta \rangle$. The refractive index of the film is then characterized by an in-plane component, n_t, and a normal-to-plane component, n_n, which are functions of the direction of the transition moment.[42] In principal the transmittance of light through a substrate covered by a uniaxially nonisotropic film can be calculated exactly, provided all refractive indexes are known.[43] In practice, n_t and n_n are difficult to measure and, as in the present case, are often not explicitly known. However, it is not necessary to know the actual absorption but rather the dichroic ratio A_s/A_p, which is much more sensitive to the chromophore orientation than is the absolute absorption. In turn A_s/A_p is much less dependent on the exact values of n_t and n_n. Therefore, following most other treatments of this problem, we have neglected the birefringence of the film and used a "pseudoisotropic" real refractive index. An additional problem in such an analysis is that the real part of the refractive index should be evaluated where A_s/A_p is measured, usually at the absorption peak, which is in the region of anomalous dispersion.[44] To avoid this, a value assumed or measured far from resonance is often used. The error introduced by this procedure is more severe for the ultraviolet–visible wavelength region than in the infrared region, where absorption coefficients are weak. By performing ellipsometry at the absorption peak we have obtained a value for the real resonant refractive index (albeit a "pseudoisotropic" one), as well as the imaginary component due to absorption. Finally, we have followed the procedure of Orrit et al.[32] (see eq 23) to account for the presence of a LB film on each side of the substrate, to correct for reflection at the various interfaces, and to be able to use an uncoated substrate as a reference. Our calibration curve of A_s/A_p as a function of $\theta_{\text{eff}} \equiv \cos^{-1}(\langle \cos^2 \theta \rangle^{1/2})$ is given in Figure 9. This was derived from a numerical computation, using an angle of 45° for incidence of light on the sample and a value for the imaginary part of the refractive index, $k = 0.07$. A series of values for the real part of the refractive index, $n = 1.55$, 1.57, and 1.59 around the ellipsometrically measured 1.58 were used in the calculation to illustrate the resulting variation in θ_{eff} for a given dichroic ratio. The values of θ_{eff} in the following discussion were all derived by using $n = 1.58$, whose calibration curve is not explicitly shown but can readily be interpolated from those in Figure 9.

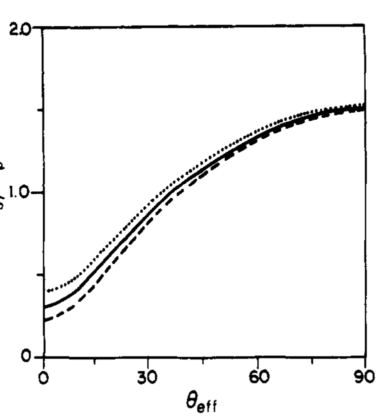

Figure 9. Theoretical dependence of the dichroic ratio of absorption, A_s/A_p, on effective polar orientation angle, θ_{eff}, for uniaxial symmetry at a 45° incident angle calculated for different real refractive indexes: $n = 1.55$ (- - -), $n = 1.57$ (—), $n = 1.59$ (· · ·).

From the ultraviolet spectra at 45° incidence we find a value of $\langle P_2 \rangle = 0.50$ at room temperature ($\theta_{\text{eff}} = 35°$), 0.30 at 70 °C, and 0.22 at 90 °C ($\theta_{\text{eff}} = 43$ and 46°, respectively). The FTIR data give additional information and confirmation of these results. Thus the polarized FTIR transmission at normal incidence also shows a dichroism prior to heating of the films. The dichroic ratio of 2.1 measured for the band at 1601 cm^{-1} polarized along the molecular axis is essentially the same as that reported in Figure 5 for the ultraviolet absorption at normal incidence. After heating to 150 °C and cooling to room temperature, the loss of this normal-incidence infrared transmission polarization not only confirms that the azobenzene chromophore loses in-plane orientation on thermal annealing but also demonstrates that all the polymer groups do so. The decrease in GIR intensity of the 1601-cm^{-1} band with increasing temperature seen in Figure 7 also indicates an increasing effective polar angle. With the room-temperature value of $\langle P_2 \rangle$ obtained from the ultraviolet spectroscopy as a reference, it can be calculated from these GIR data that heating from 25 to 150 °C increased θ_{eff} by 11° and heating to 100 °C (not shown) increased θ_{eff} by 9°. These results are essentially identical with the 11° increase in θ_{eff} on heating from 25 to 90 °C that can be calculated from the ultraviolet dichroism in Figure 5. However, as seen above, an increase in θ_{eff} by only 11° from an initial value of 35° decreases the value of $\langle P_2 \rangle$ by a factor of 2. In fact, as discussed in section 4.4, this change in θ_{eff} on heating may represent not a real change in average molecular orientation but rather a broadening of the distribution function $N(\theta)$.

4.3. Thermal Stability. As noted in the Results, on heating a Langmuir–Blodgett film of the copolymer $x = 5$ to 150 °C and cooling the film back to room temperature, the GIR intensities of all the bands and therefore orientation of the entire film structure return to their values prior to the heat cycle. (The first heating cycle is an exception to this observation. This is understandable in terms of the irreversible in-plane randomization that occurs on the initial heating as already discussed in the preceding section.) In fact, not only GIR reflection but also ultraviolet dichroism and ellipsometry are all consistent in showing that the chromophoric order and film structure in these polymeric Langmuir–Blodgett films has substantial thermal stability. A similar conclusion has been reported for amphiphilic polymers with hydrophilic spacers and hydrocarbon or fluorocarbon side chains.[26,29] In the present instance, the GIR experiments demonstrate that not only the polymer backbone and spacer groups but also chromophores resist permanent disordering on heating to 150 °C. For the polymer $x = 5$ this is more than 60 °C above its bulk clearing temperature. Indeed, optical microscopy of Langmuir–Blodgett films of this polymer do not give any indication of film disruption (e.g., droplet formation) to at least 200 °C although the edges of scratches deliberately made in the film form visible liquid droplets.

The spectroscopy and ellipsometry show that both integral film structure and molecular ordering are retained. Clearly the intermolecular cohesion is much higher in these films than in the bulk material.[26,45] The reason for this enhanced stability is not entirely clear. In addition to a more confined molecular structure resulting in enhanced intermolecular cohesion forces including hydrogen bonding, it is possible that chemical cross-linking through transesterification may occur at an elevated temperature, as has recently been observed for HEA-based copolymers in bulk.[46]

4.4. Phase Change. A striking feature of the thermal behavior of these Langmuir–Blodgett films of polymer $x = 5$ is that several distinct but related properties change abruptly at about 60 °C. These are (1) the irreversible annealing out of in-plane molecular order induced by the deposition process, (2) the reversible change in axial chromophoric orientation as monitored by $\langle P_2 \rangle$, and (3) a reversible shift in the absorption peak position. All three can be explained by an increase in molecular mobility at this temperature, allowing a restructuring of the film—in effect a phase transition. Reversibility is an important characteristic of a true phase change and is exhibited by observations 2 and 3 but not by 1. Since this in-plane orientation is ascribed to flow-induced shear forces during deposition, it is not surprising that its relaxation is irreversible. These forces are no longer present in the deposited film. In-plane order caused by intermolecular interactions generally extends over too small a distance to be detected by these macroscopic probes.[16] In contrast, axial order needs only to span an individual monolayer width since the same axial structure is presumably repeated in each layer. (For the first few layers many materials show a change in order with film thickness,[47] but our experiments used a minimum of nine layers.) Thus the molecularly induced axial order in the films can be monitored by these techniques. Thermally induced disordering causes a loss in intermolecular structure manifested as a decrease in the order parameter. The change in the chromophore absorption band position with temperature shown in Figure 5 supports this picture. The peak seen at 335 nm around room temperature is well-known to be an excitonic band generated by the intermolecular dipolar coupling of adjacent azobenzene molecules, that is, an aggregation effect.[48,49] The hypsochromic nature of this band relative to the chromophore in dilute solution results from the symmetric face-to-face packing of the chromophores. Within the context of the point-dipole model of such aggregation, the chromophores must be tilted less than 35.3° from the normal to the film plane to exhibit a hypsochromically allowed transition.[50] At greater tilt angles the additional lower energy band resulting from the dipolar interaction is symmetry allowed and becomes the dominant band observed. This is a rather crude model, and the coincidence with our measured value of 35° for θ_{eff} at room temperature is largely coincidental. But, if the value of ca. 45° for θ_{eff} derived from the dichroism at higher temperature actually represented a closely ordered array of chromophores with this tilt angle, an aggregate band shifted bathochromically from the molecular absorption should be observable, a so-called J aggregate as has in fact been seen for some azobenzene systems in other media.[51] However, in the present case the band at 355 nm seen above 60 °C can be identified with molecular or nonaggregated π–π^* absorption of the azobenzene chromophore based on its similar peak wavelength position to dilute solution spectra. The picture that emerges is shown schematically in Figure 10. At low temperature the chromophores within a domain are highly ordered, aggregated, and tilted about 35° from the normal. In this case the distribution of orientations is probably quite narrow or well-defined aggregation would not occur.[52] Above the transition temperature there is more disorder in the film. Although the chromophores are still largely oriented in a common direction, the packing has become sufficiently loose that aggregation no longer occurs. It is important to recognize that a decrease in the order parameter $\langle P_2 \rangle$ does not require the molecules all to undergo a substantial increase in tilt. It is sufficient for the *distribution* of orientations to broaden without the average tilt angle necessarily increasing. Mathematically this can come about since $\langle P_2 \rangle$ is a linear function of $\langle \cos^2 \theta \rangle$ rather than of $\langle \cos \theta \rangle$. Thus the *average* tilt angles above and below 60 °C may not differ appreciably. This is supported by ellipsometry measured as a function of temperature. Ellipsometry is directly sensitive to average molecular tilt, that is, it is proportional to $\langle \cos \theta \rangle$. As seen in Figure 6 there is no discernible break in the slight downward trend in film thickness with increasing temperature in the vicinity of 60 °C where the largest change in $\langle P_2 \rangle$ occurs. In fact, the overall change in thickness between room temperature and 150 °C monitored during the second heating cycle after the initial annealing shows only a change of 4 Å in film thickness, a reduction of slightly more than 1%. Taking $\theta_{\mathrm{eff}} = 35°$ at room temperature from the ultraviolet spectroscopy, an angle of 46° is calculated at 150 °C from the ellipsometric data of the second heating cycle. If the change in θ_{eff} of 11° on heating to 150 °C measured from the GIR data were actually entirely due to an increase in tilt from 35 to 46°, the film thickness should have decreased by 49 to 271 Å. Since the overall observed change is only about 10% of this, we attribute the decrease in $\langle P_2 \rangle$ on heating primarily to a broadening of the distribution of title angles with little change in the average value.

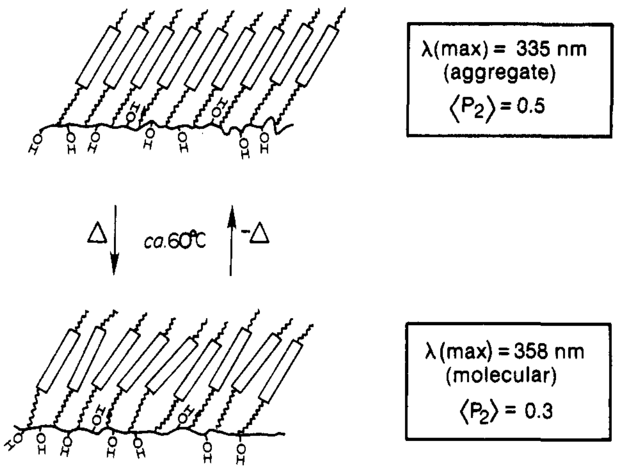

Figure 10. Schematic representation of thermally induced order–disorder transition in a Langmuir–Blodgett film domain of an amphotropic polymer.

We believe it is highly significant that the transition temperature at which this increased mobility and decreased order occur in the Langmuir–Blodgett films is essentially the same as the bulk crystal to liquid crystal phase-transition temperature. In both cases an increase in molecular mobility occurs with a partial but reversible decrease in molecular order.

5. Conclusions

The ordering and thermal behavior of thermotropic and amphiphilic (i.e., amphotropic) polymers containing azobenzene mesogenes have been investigated in monolayers at the air–water interface and in Langmuir–Blodgett multilayers. We have demonstrated that the film-forming and deposition properties of these polymers can be adjusted by the incorporation of varying amounts of a hydrophilic comonomer. Ultraviolet and infrared spectroscopy show that the chromophoric groups are highly oriented. In-plane ordering caused by the deposition process is eliminated by mild heating, without destroying axial orientation. A reversible thermal transition to a less-ordered state occurs at the same temperature in the Langmuir–Blodgett film as the bulk crystal to liquid crystal phase transition. It has been possible to impart mobility to the molecular subunits in the films through heating without irreversibly destroying the order and structure. In fact, the Langmuir–Blodgett films can be heated far beyond the material's bulk isotropic clearing temperature while retaining substantial molecular order. On subsequent cooling to below the transition temperature a highly ordered molecular structure is repeatedly recovered. These properties hold the promise of using external forces such as an electric field to induce large-scale ordering of the molecules while in a mobile phase and then to stabilize this monodomain structure by cooling,[12] as can already be done with bulk liquid-crystalline materials.[53]

Acknowledgment. We thank C. Urban, University of Mainz, for providing the azobenzene monomer. We gratefully acknowledge the contributions of the following individuals at the Research Laboratories of Eastman Kodak Co. R. Aust performed the ellipsometry measurements at 350 nm. J. Littman and S. Van Slyke provided the aluminized silicon substrates. V. DePalma kindly provided advice and his plans for constructing the heater for the infrared spectrometer. H.R. and A.S. acknowledge support by the German Ministry of Research and Technology (BMFT-Project No. 03 M 4008 F1).

References and Notes

(1) Breton, M. *J. Macromol. Sci. Rev. Macromol. Chem.* **1981**, *C21*, 61–87 and references therein.

(2) Tredgold, R. H.; Winter, C. S. *J. Phys. D: Appl. Phys.* **1982**, *15*, L55–58.

(3) Tredgold, R. H. *Thin Solid Films* **1987**, *152*, 223–230 and references therein.

(4) Elbert, R.; Laschewsky, A.; Ringsdorf, H. *J. Am. Chem. Soc.* **1985**, *107*, 4134–4141.

(5) Tredgold, R. H.; Vickers, A. J.; Hoorfar, A.; Hodge, P.; Khoshdel, E. *J. Phys. D: Appl. Phys.* **1985**, *18*, 1139–1145.

(6) Mumby, S. J.; Swalen, J. D.; Rabolt, J. F. *Macromolecules* **1986**, *19*, 1054–1059.

(7) Laschewsky, A.; Ringsdorf, H.; Schmidt, G.; Schneider, J. *J. Am. Chem. Soc.* **1987**, *109*, 788–796.

(8) Biddle, M.; Lando, J. B.; Ringsdorf, H.; Schmidt, G.; Schneider, J. *J. Colloid Polym. Sci.* **1988**, *266*, 806–813.

(9) Tredgold, R. H.; Young, M. C. J.; Jones, R.; Hodge, P.; Kolinsky, P.; Jones, R. J. *Electron. Lett.* **1988**, *24*, 308–309.

(10) Hall, R. C.; Lindsay, G. A.; Anderson, B.; Kowel, S. T.; Higgins, B. G.; Stroeve, P. *Mater. Res. Soc. Symp. Proc.* (*Nonlinear Opt. Prop. Polym.*) **1988**, *109*, 351–356.

(11) Erdelen, C.; Laschewsky, A.; Ringsdorf, H.; Schneider, J.; Schuster, A. *Thin Solid Films* **1989**, *180*, 153–166.

(12) Ringsdorf, H.; Schlarb, B.; Venzmer, J. *Angew. Chem., Int. Ed. Engl.* **1988**, *27*, 113–158.

(13) Hodge, P.; Khoshdel, E.; Tredgold, R. H.; Vickers, A. J.; Winter, C. S. *Brit. Polym. J.* **1985**, *17*, 368–371.

(14) Tieke, B.; Graf, H.-J.; Wegner, G.; Naegele, B.; Ringsdorf, H.; Banerjie, A.; Day, D.; Lando, J. B. *Colloid Polym. Sci.* **1977**, *255*, 521–531.

(15) Veale, G.; Peterson, I. R. *J. Colloid Interface Sci.* **1985**, *103*, 178–189.

(16) Garoff, S.; Deckman, H. W.; Dunsmuir, J. H.; Alvarez, M. S.; Bloch, J. M. *J. Phys.* **1986**, *47*, 701–709.

(17) Fischer, A.; Sackmann, E. *J. Phys.* **1984**, *45*, 517–527.

(18) Rucha, B. U.; Rabe, J.; Schneider, G.; Knoll, W. *J. Colloid Interface Sci.* **1986**, *114*, 1–8.

(19) Jones, R.; Tredgold, R. H.; Hoorfar, A.; Allen, R. A.; Hodge, P. *Thin Solid Films* **1985**, *134*, 57–66.

(20) Schuster, A. Diplomarbeit, Universität Mainz, 1986.

(21) Ringsdorf, H.; Urban, C. To be published.

(22) Allara, D. L.; Swalen, J. D. *J. Phys. Chem.* **1982**, *86*, 2700–2704.

(23) Schlotter, N. E.; Rabolt, J. F. *Appl. Spectrosc.* **1985**, *39*, 994–996.

(24) Frick, G.; Ringsdorf, H.; Schuster, A.; Wendorff, J. H. To be published.

(25) Rabolt, J. F.; Burns, F. C.; Schlotter, N. E.; Swalen, J. D. *J. Chem. Phys.* **1983**, *78*, 946–952.

(26) Schneider, J.; Ringsdorf, H.; Rabolt, J. F. *Macromolecules* **1989**, *22*, 205–210.

(27) Kübler, R.; Lüttke, W.; Weckherlin, S. *Z. Elektrochem.* **1960**, *64*, 650–658.

(28) Diele, S.; Oelsner, S.; Kuschel, F.; Hisgen, B.; Ringsdorf, H.; Zentel, R. *Makromol. Chem.* **1987**, *188*, 1993–2000.

(29) Schneider, J.; Erdelen, C.; Ringsdorf, H.; Rabolt, J. F. *Macromolecules* **1989**, *22*, 3475–3480.

(30) Ringsdorf, H.; Schneller, A. *Brit. Polym. J.* **1981**, *13*, 43–46.

(31) Michl, J.; Thulstrup, E. W. *Spectroscopy with Polarized Light*; VCH Publishers: Deerfield Beach, FL, 1986.

(32) Orrit, M.; Möbius, D.; Lehmann, U.; Meyer, H. *J. Chem. Phys.* **1986**, *85*, 4966–4979.

(33) Schellman, J.; Jensen, H. P. *Chem. Rev.* **1987**, *87*, 1359–1399.

(34) Chollet, P.-A. *Thin Solid Films* **1978**, *52*, 343–360.

(35) Blinov, L. M.; Dubinin, N. V.; Mikhnev, L. V.; Yudin, S. G. *Thin Solid Films* **1984**, *120*, 161–170.

(36) Francis, S. A.; Ellison, A. H. *J. Opt. Soc. Am.* **1959**, *49*, 131–138.

(37) Allara, D. L.; Nuzzo, R. G. *Langmuir* **1985**, *1*, 52–66.

(38) Nakahara, H.; Fukuda, K. *J. Colloid Interface Sci.* **1979**, *69*, 24–33.

(39) Daniel, M. F.; Hart, J. T. T. *J. Mol. Electron.* **1985**, *1*, 97–104.

(40) Jaffé, H. H.; Orchin, M. *Theory and Applications of Ultraviolet Spectroscopy*; Wiley: New York, 1962; p 280.

(41) Vandevyver, M.; Barraud, A.; Ruaudel-Teixier, A.; Maillard, P.; Gianotti, C. *J. Colloid Interface Sci.* **1982**, *85*, 571–585.

(42) Explicitly, the equations for the nonzero elements of the dielectric tensor under uniaxial symmetry can be written as

$$\epsilon_{xx} = \epsilon_{yy} = \epsilon_{xx}{}^{r} + 4\pi i p(1 - \langle\cos^2\theta\rangle)/2$$
$$\epsilon_{zz} = \epsilon_{zz}{}^{r} + 4\pi i p\langle\cos^2\theta\rangle$$

where ϵ_{jj} are the components of the dielectric tensor with z as the uniaxial axis normal to the film plane, $\epsilon_{jj}{}^{r}$ are the real components of the dielectric constant, and p contains contributions of the transition dipole, local field factors, and density.[31] Refractive index components are related to the dielectric constant elements by

$$n_{t} = (\epsilon_{xx})^{1/2} \qquad n_{n} = (\epsilon_{zz})^{1/2}$$

(43) Mosteller, L. P.; Wooten, F. *J. Opt. Soc. Am.* **1968**, *58*, 511–518.

(44) Wooten, F. *Optical Properties of Solids*; Academic Press: New York, 1972; p 47.

(45) Rothberg, L.; Higashi, G. S.; Allara, D. L.; Garoff, S. *Chem. Phys. Lett.* **1987**, *133*, 67–72.

(46) Plage, B.; Schulten, H.-R.; Ringsdorf, H.; Schneider, J. *Macromolecules*, in press.

(47) Bonnerot, A.; Chollet, P. A.; Frisby, H.; Hoclet, M. *Chem. Phys.* **1985**, *97*, 365–377.

(48) Heesemann, J. *J. Am. Chem. Soc.* **1980**, *102*, 2167–2176.

(49) Fukuda, K.; Nakahara, H. *J. Colloid Interface Sci.* **1984**, *98*, 555–564.

(50) Kasha, M. *Spectroscopy of the Excited State*; DiBartolo, B., Ed.; Plenum: New York, 1976; pp 337–363.

(51) Shimomura, M.; Ando, R.; Kunitake, T. *Ber. Bunsen-Ges. Phys. Chem.* **1983**, *87*, 1134–1143.

(52) Kimizuka, N.; Kunitake, T. *Chem. Lett.* **1988**, 827–830.

(53) Ringsdorf, H.; Zentel, R. *Makromol. Chem.* **1982**, *183*, 1245–1256.

Registry No. I (homopolymer), 131681-79-3; I(HEA) (copolymer), 131681-80-6.